A Mechanism for Rotamase Catalysis by the FK506 Binding Protein (FKBP)†

Stefan Fischer, Stephen Michnick, and Martin Karplus*

Department of Chemistry, Harvard University, 12 Oxford Street, Cambridge, Massachusetts 02138

Received July 12, 1993; Revised Manuscript Received September 20, 1993•

ABSTRACT: A detailed mechanism for the catalysis of prolyl isomerization by the rotamase enzyme FKBP is proposed on the basis of a model constructed from the known structure of the FK506/FKBP complex. The model substrate is bound as a type VIa proline turn with the ends exposed to permit longer polypeptide chains (e.g., protein loops) to act as substrates. An *ab initio* potential for the isomerized imide bond is combined with a molecular mechanics representation of the rest of the system to calculate the reaction path. The resulting activation energy for the enzymatic *cis* → *trans* isomerization is equal to about 6 kcal/mol, in good agreement with experiment. The lowering of the barrier relative to the solution value of 19 kcal/mol is found to arise from a combination of desolvation of the imide carbonyl, ground-state destabilization, substrate autocatalysis, and preferential transition-state binding. Minimal rearrangements are required in the enzyme and the substrate along the reaction path. The enzyme residues that participate in catalysis agree with the available mutation data. The type VIa turn model corresponds to a sequence-specific structural motif commonly found on the surface of proteins. It is likely to have a role in the formation of protein complexes with FKBP-like domains that function as foldases or chaperones.

FK506 binding proteins (FKBPs) constitute one of the two known classes of peptidylprolyl isomerases (PPIases), also known as rotamases (Trandinh *et al.*, 1992). The other class of PPIases is composed of the cyclophilins, which are named for their high affinity for cyclosporin A. FK506 and cyclosporin A are macrocyclic ligands which inhibit the rotamase activity of their respective class, while leaving the other class unaffected. Because both of these inhibitors act as immunosuppressants, significant effort has gone into understanding their interactions with the binding proteins and the effect of the complex on the immune system (Schreiber, 1991). Although there is no evidence that inhibition of the PPIase activity is related to immunosuppression (Schreiber & Crabtree, 1992), the rotamase reaction is of interest in itself and because PPIases accelerate the folding of proteins (Fischer *et al.*, 1989; Tropschug *et al.*, 1990) for which the rate-limiting step involves the *trans* → *cis* isomerization of proline peptide bonds (Brandts *et al.*, 1975). The presence of PPIases in the cells of many organisms suggests that they have a role as foldases and chaperones *in vivo* (Fischer & Schmid, 1990; Freedman, 1992; Gething & Sambrook, 1992; Tai *et al.*, 1993).

The catalytic mechanism of prolyl isomerization by the PPIases has not been established. A variety of mechanistic proposals have been made, and some of them have been excluded or supported by experiment; a detailed review of the current status is given by Stein (1993). It has been demonstrated that catalysis is unlikely to be based on a covalent intermediate (Kofron *et al.*, 1991; Park *et al.*, 1992), as originally proposed by Fischer *et al.* (1989). Substrate desolvation (Wolfenden & Radzicka, 1991; Eberhardt *et al.*, 1992) and substrate distortion (Harrison & Stein, 1990a; Rosen *et al.*, 1990) are thought to be involved in the catalysis, and secondary deuterium isotope effect data are consistent with their role (Harrison & Stein, 1992; Stein, 1993). Quantitative values of the relative contributions to catalysis are not available from experiment. It is here that theory can supplement the experimental data, as we show in this paper. Measurements by Albers *et al.* (1990)[1] of the catalysis of the *cis* → *trans* isomerization of leucylprolyl model substrates by FKBP have shown that the activation enthalpy is near 5.5 kcal/mol, about 13.5 kcal/mol lower than the solution value. The decrease in the free energy of activation, $\Delta\Delta G^{\ddagger}$, relative to the uncatalyzed reaction, was measured to be 6.2 kcal/mol. This is in agreement with most other values found for $\Delta\Delta G^{\ddagger}$, e.g., the value of 6.7 kcal/mol from Kofron *et al.* (1991) and of 6.6 kcal/mol from Park *et al.* (1992).

A molecular mechanics calculation (Brooks *et al.*, 1988; Bash *et al.*, 1991) augmented by *ab initio* results has been used to make a theoretical analysis of the FKBP rotamase mechanism and estimate the contribution of different factors to catalysis. A model of the bound peptide substrate has been constructed on the basis of the X-ray structure of the FKBP/FK506 complex (Van Duyne *et al.*, 1991, 1993) on the assumption that a portion of FK506 mimics the transition state (Figure 1A). The blocked tetrapeptide *N*-acetyl-Leu-Pro-Phe-methylamide (Figure 1B), a fragment of the preferred experimental substrate (Harrison & Stein, 1990b; Albers *et al.*, 1990), was used for the study. From the FKBP/FK506 complex structure and molecular modeling, the peptide was found to bind as a type VIa proline turn with exposed ends (Fischer, 1992), as would be required if the turn were part of a protein. An adiabatic reaction path for the *cis* → *trans* isomerization of the substrate in the enzyme was determined with a method that does not require a predefined reaction coordinate (Fischer & Karplus, 1992). The calculated *cis* →

† Supported in part by a grant from the National Institutes of Health and a gift from Molecular Simulations, Inc.

• Abstract published in *Advance ACS Abstracts*, November 15, 1993.

[1] The kinetic parameters, $\Delta H^{\ddagger}$ and $\Delta S^{\ddagger}$, published by Albers *et al.* (1990) were based on k_c/K_m. M. W. Albers, S. Schreiber, and M. Karplus (unpublished results) have corrected the original values by using the temperature dependence of k_c; k_c was determined from the original k_c/K_m values by use of the measured K_m = 0.5 mM obtained by Park *et al.* (1992) and Kofron *et al.* (1991). The correction changes only $\Delta S^{\ddagger}$, while $\Delta H^{\ddagger}$, which is of primary interest here, is the same as given in Albers *et al.* (1990).

0006-2960/93/0432-13830$04.00/0

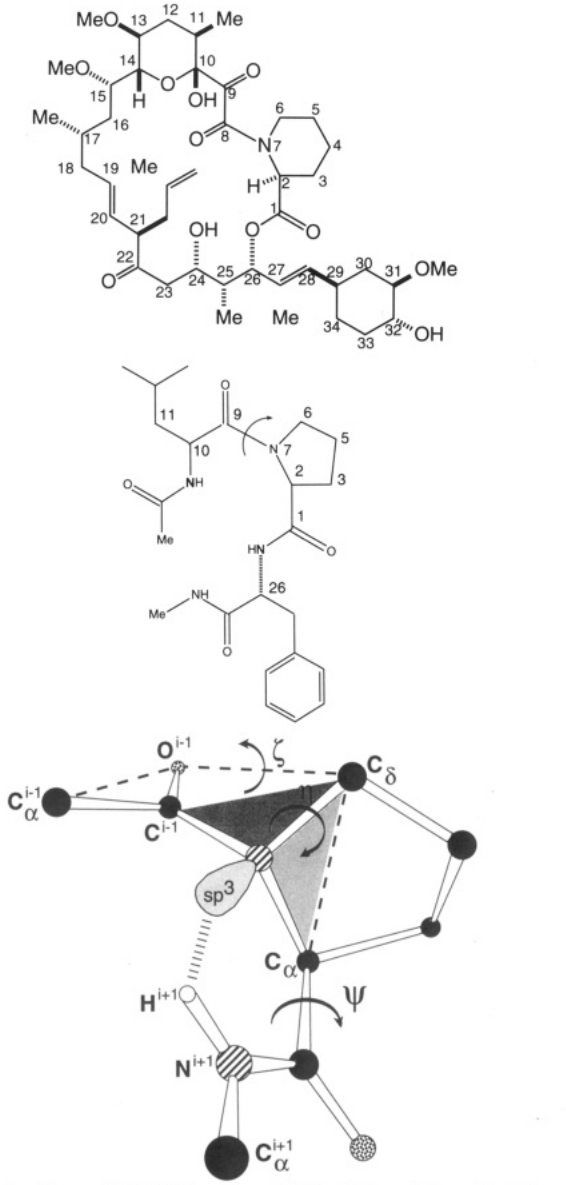

FIGURE 1: (A, top) FK506. (B, middle) *N*-Acetyl-Leu-Pro-Phe-methylamide substrate used for the calculations. The atom numbering shows the correspondence used for the initial scaffold of the substrate onto FK506. The arrow indicates the imide bond undergoing *cis* → *trans* isomerization. (C, bottom) Peptidylproline fragment in the *syn* transition state, showing the dihedral angles ζ (C_α^{i-1}–O^{i-1}–C_δ^{Pro}–C_α^{Pro}), η (C^{i-1}–C_α^{Pro}–N^{Pro}–C_δ^{Pro}, i.e., the angle between the two shaded planes), and ψ^{Pro}, as well as the sp^3 nitrogen lone pair interacting with the down-chain amide hydrogen.

trans activation barrier, $\Delta E_{cat}^{\ddagger}$, is about 6 kcal/mol, close to the experimental value found by Albers and co-workers (1990). An analysis of the calculated contributions to the barrier reduction shows that it is due to a combination of substrate desolvation, ground-state destabilization, substrate autocatalysis, and preferential transition-state binding. Mutation studies of the effect of amino acid substitutions on catalysis are consistent with the residues that are found to be important in the proposed mechanism.

METHODS

The calculations were performed with the CHARMM program (Brooks *et al.*, 1983) and the GAUSSIAN program (Frisch *et al.*, 1992). The standard CHARMM 22 all-hydrogen empirical energy function was used for most of the system (A. MacKerell *et al.*, to be published).[2] The proline imide torsion barrier and the structural change in the neighborhood of the imide bond during isomerization were corrected on the basis of *ab initio* calculations because the standard force field is not designed for large deviations from the planar *cis* or *trans* state. A 3-21G//6-31G* *ab initio* adiabatic energy map,[3] $E_{6\text{-}31G^*}(\zeta,\psi^{Pro})$, was calculated for the proline dipeptide as a function of the imide torsion angle ζ and the peptide angle ψ^{Pro} (Fischer, 1992). The angle ζ is used instead of the standard peptide bond angle ω to describe the imide bond torsion, so as to uncouple it from the pyramidalization of the imide nitrogen, which is measured by the improper dihedral angle η (see Figure 1C).[4] A correction term for the energy defined by

$$\Delta E_{correct}(\zeta,\psi^{Pro}) = E_{6\text{-}31G^*}(\zeta,\psi^{Pro}) - E_{CHARMM}(\zeta,\psi^{Pro})$$

relative to the *trans* minimum was employed; here $E_{CHARMM}(\zeta,\psi^{Pro})$ was obtained from the CHARMM potential energy function for the proline dipeptide.

In all calculations, the substrate and the 23 residues of FKBP delimiting the binding pocket (Van Duyne *et al.*, 1991, 1993; i.e., residues 25–27, 36–39, 42, 46–48, 54–56, 59, 81–82, 86–87, 90–91, 97, and 99) were free to move, and residues 1–24, 63–80, 94–96, 98, and 100–107 were kept fixed. The remaining FKBP residues form a layer between the fixed and the free regions and were harmonically constrained to their positions in the crystal structure with force constants corresponding to the experimental temperature factors.

Standard protonation states were used for all residues except for the histidines. The pK_a's of His25, His87, and His94 were determined with the continuum electrostatic method (Bashford & Karplus, 1990) to be 6.15, 6.84, and 6.79, respectively; these values were essentially unaffected by the binding of the substrate. Examination of the electrostatic interaction energy between the side chains of each of these histidines and the rest of the system showed that the singly ϵ-protonated residue was most stable in all three cases; this form was used in the present study.

To account for solvent shielding of the electrostatic interactions, a continuum dielectric calculation was done for the transition state of the FKBP/substrate complex with the UHBD program (Davis & McCammon, 1990); for the interior of the complex a dielectric constant $\epsilon_{int} = 1$ was used, while bulk water was treated with $\epsilon_{ext} = 78.5$. The interaction energy, U_i, between the substrate and each residue i of FKBP, calculated from the continuum model as described by Gilson and Honig (1988), was compared with the corresponding unshielded electrostatic interaction energy, E_i, obtained from the CHARMM program. The ratio between the two yields an effective residue-specific dielectric constant, $\epsilon_i^{eff} = E_i/U_i$ (Bashford & Karplus, 1990). In the calculations, the electrostatic interaction energies were computed with the charges of each enzyme residue i scaled by ϵ_i^{eff}; the substrate charges were not scaled. This approach approximates the

[2] A full set of parameters is given in the CHARMM 22 program; for details, inquire from the corresponding author.

[3] In the adiabatic calculations, the geometries were fully optimized at the 3-21G level over a grid of fixed values of the ζ and ψ^{Pro} angles; energies were then reevaluated at the 6-31G* level. Full optimization of the proline dipeptide at the 6-31G* level for the *cis*, *trans*, *syn*, and *anti* structures yielded very similar results (deviations of less than 0.27 kcal/mol).

[4] The angles ζ and η have the values $(\zeta,\eta)_{cis} = (0, 180)$ and $(\zeta,\eta)_{trans} = (180, 180)$ for the planar *cis* and *trans* structures and the values $(\zeta,\eta)_{syn}^{\ddagger} \approx (+90, \pm 120)$ and $(\zeta,\eta)_{anti}^{\ddagger} \approx (-90, \pm 120)$ for the pyramidal transition states. For $\eta = 180°$, all atoms attached to the nitrogen are in a plane; for $\eta = \pm 120°$; the nitrogen is tetrahedral.

solvent shielding effects for a substrate interacting with the protein and is fast enough to make possible the optimization and reaction path calculations. It should be accurate as long as changes in the protein structure are small, as is true in the present case.

Substrate Docking and Reaction Path Determination. An essential part of the calculation is the docking of the substrate and the determination of the reaction path connecting the *cis* to the *trans* isomer. The model substrate *N*-acetyl-Leu-Pro-Phe-methylamide (Albers *et al.*, 1990; Harrison & Stein, 1990b) was used; neutral blocking groups were included to avoid artifacts from charged peptide termini. To dock the substrate, it was assumed that the bound FK506 in the FK506/FKBP crystal structure (Van Duyne *et al.*, 1991, 1993) mimics the *syn* transition-state structure[4] of a peptidylprolyl substrate (Albers *et al.*, 1990; Rosen *et al.*, 1990). The six-membered pipecolinyl ring of FK506 (atoms 2–7 in Figure 1A) resembles the proline ring, and the C9 α-keto carbonyl is oriented relative to the ring as would be the imide carbonyl of a prolyl peptide twisted in the *syn* form. The substrate was docked to FKBP by scaffolding the imide group and proline ring onto the corresponding groups of FK506. Three substrate conformers, called here syn_{90}^{ini}, cis_ζ, and $trans_\zeta$, were constructed by the following procedure. First, an approximate transition-state structure with $\zeta = 90°$, syn_{90}^{ini}, was determined by assigning the atoms of the proline dipeptide moiety of the substrate to the positions of atoms in FK506, according to the numbering in Figure 1B. The two terminal peptide groups of the substrate, which have no direct correspondence in FK506, were oriented manually so as to maximize the number of hydrogen bonds. This positions the C_β atoms of the Leu and Phe side chains; they were fitted into the site so as to bury the hydrophobic Leu side chain and to optimize the interactions of the Phe side chain with Phe 46 and Phe 48 of FKBP. The syn_{90}^{ini} model was then partially optimized by minimizing the energy of the complex while constraining ζ to 90°. Starting from the new syn_{90}^{ini} complex structure, gradual displacement of the constraint on ζ to 90 ± 40°, followed by complete relaxation of the system in the absence of any constraint on ζ, yielded the cis_ζ and $trans_\zeta$ conformers (see Table I for geometries). The cis_ζ and $trans_\zeta$ structures were found to be the minima on the two sides of the barrier. In addition, there is a local minimum, $trans_{180}$, closer to the planar geometry.

The minimum energy path connecting the reactant *cis* to the product *trans*, was calculated with the *c*onjugate *p*eak *r*efinement (CPR) algorithm (Fischer & Karplus, 1992) implemented in the *t*rajectory *r*efinement *a*lgorithm (TRAVEL) module of the CHARMM program. The results of the calculation are a set of structures (between 50 and 80 in the present analysis) of the enzyme/substrate complex along a curvilinear path from the reactant via the transition state to the product. Convergence of the path refinement is achieved when all the local energy maxima along the path are exact saddle points. The advantage of the CPR algorithm is that the results are not biased by the choice of a preselected reduced reaction coordinate, such as ω or ζ. Instead, all the atoms of the substrate (65) and the moving atoms of FKBP (807) included in the calculation could contribute to the reaction coordinate. The path was computed by providing the cis_ζ and $trans_\zeta$ conformers as the reactant and product. The structure, syn_{90}^{ini}, was used as the first guess for the transition state to ensure that a *syn* rather than an *anti* pathway would be refined, in accord with the C9 α-keto carbonyl orientation of bound FK506. Syn_{90}^{ini} was replaced by an improved structure, syn_{90}, by the refinement procedure. The $trans_\zeta$ to $trans_{180}$ path was also determined with the CPR method. Finally, the cis_ζ path was extended to $\zeta = 0°$ by adiabatically decrementing ζ in steps of 5°. To refine the reaction path, the CPR results were optimized with an improved version (synchronous chain minimization, SCM) of the method of Choi and Elber (1991).

Table I: Soft Backbone Torsion Angles (deg) and Imide Group Deformation Angles (deg) of the Bound Substrate[a]

	type VIa turn			
	cis_ζ	syn_{90}	$trans_\zeta$	$trans_{180}$
ϕ^{Leu}	−103 (2)	−97 (1)	−123 (15)	−83 (2)
ψ^{Leu}	116 (5)	64 (3)	56 (13)	−46 (1)
ϕ^{Pro}	−109 (1)	−119 (2)	−109 (3)	−84 (3)
ψ^{Pro}	38 (2)	14 (1)	14 (5)	65 (1)
ϕ^{Phe}	−73 (2)	−70 (2)	−84 (1)	−108 (6)
ψ^{Phe}	146 (1)	145 (3)	146 (2)	150 (3)
ζ	25 (7)	90	137 (1)	200 (2)
η	−153 (1)	−129 (1)	−165 (3)	−168 (2)

[a] In parentheses are variations that result from alternate orientations of the Leu and Phe side chains of the substrate. See Figure 1C and text for definitions of conformations and angles.

RESULTS

The substrate is bound as a type VIa proline turn with an intrasubstrate hydrogen bond between the N–H of Phe and the C=O of the *N*-acetyl group at the amino terminus so as to form a 10-membered ring (Fischer, 1992). Type VIa proline turns are commonly found on the surface of proteins with *cis* prolines in the "*i* + 2" position (Richardson & Richardson, 1989; Müller *et al.*, 1993); the backbone torsion angle ψ^{Pro} in such a turn has the ideal value of 0° and is observed to be in the −20° to 45° range (McArthur & Thornton, 1991). Figure 2 shows the calculated results for the tetrapeptide bound to FKBP at three successive stages along the reaction path: the reactant cis_ζ, the intermediate point syn_{90}, and the product $trans_\zeta$. In what follows we use the syn_{90} structure, rather than the transition state (see below), to analyze the results because it is near the maximum of the substrate energy along the reaction path. Table I gives the backbone torsion angles of the substrate in the different states. The dihedral angles for the cis_ζ, syn_{90}, and *trans* conformers correspond to those of a type VIa turn. The intrasubstrate hydrogen bond is broken in $trans_\zeta$ and in $trans_{180}$. Another intrasubstrate H-bond is formed in $trans_{180}$ between the Phe amide hydrogen and the Leu imide carbonyl. All three stable conformers have a twisted imide bond. The cis_ζ and $trans_\zeta$ conformers are distorted toward the *syn* transition state, with $\zeta \approx 25°$ and $\zeta \approx 137°$, respectively, while $trans_{180}$ is twisted away from it with $\zeta \approx 200°$. The imide nitrogen pyramidalization[2] is maximal at syn_{90} with $\eta \approx -129°$; the *cis* and *trans* states have a nearly planar nitrogen with η values between −168° and −153°.

During the reaction, the positioning of the proline ring relative to FKBP remains essentially the same as that of the pipecolinyl ring of FK506. The Leu side chain extends in the direction of the CH_3 group of methylene C11 in FK506 (see Figure 1). The dihedral angle χ_1^{Leu} is in a staggered position, and the side chain is located beneath His 87 in a hydrophobic pocket formed by Ile 90 and Ile 91. The dihedral angle χ_2^{Leu} can adopt any staggered values. The Phe side chain, whose ring has several possible positions, can occupy a groove formed by Phe 46, Phe 48, and Glu 54 (not shown) or lie flat over the ring of Phe 46 (as in Figure 2). These variations have only minor effects on the rest of the substrate structure or on the reaction mechanism. The structure of FKBP with the bound substrate is very similar to the FKBP/FK506 cocrystal structure. The only significant deviation is in the orientation of the Tyr 82 hydroxyl, which points outward and

interacts with the Phe carbonyl group of the substrate, rather than inward as it does when interacting with the C8 imide carbonyl of FK506.

Enzyme/Substrate Interactions. Figure 3 shows the hydrogen bonding of six of the seven potential donors or acceptors of the tetrapeptide. There is the intrasubstrate hydrogen bond already described, and there are four hydrogen bonds between the substrate and the enzyme. Two of the hydrogen bonds, from the proline carbonyl to the N—H of Ile 56 and from the C-terminal N—H of the substrate to the carbonyl of Glu 54, form a short stretch of antiparallel twisted β-sheet between the enzyme and substrate backbones. The other two are from the N—H of Leu to the side-chain carboxyl of Asp 37 and, as already mentioned, from the C=O of Phe to the hydroxyl group of Tyr 82. These four H-bonds are maintained throughout the reaction path, as can be seen from the distances listed in Table II. All four enzyme groups that are partners of these hydrogen bonds to the substrate are involved in hydrogen bonds to FK506 in the cocrystal structure [see Table II and Van Duyne *et al.* (1991, 1993)]. The hydrogen bond geometries in the FKBP/tetrapeptide model are comparable to those of the FKBP/FK506 complex. Three of the hydrogen bonds form a chain across the binding site (those involving the Leu amide, the Phe amide, and the Ile 56 amide) with the dipole moments of all three amide groups favorably aligned along the chain. The intrasubstrate hydrogen bond, which gives the characteristic type VIa turn conformation to the tetrapeptide, is stabilized by the orientation of the N-terminal amide and the Phe amide of the substrate required for making hydrogen bonds with Asp 37 and Ile 56. Only the imide carbonyl of the substrate makes no strong hydrogen bonds at any stage along the reaction path, though it is involved in weakly polar interactions with C—H bonds of the aromatic triad Tyr 26, Phe 36, and Phe 99 (Desiraju, 1991). The position of the imide carbonyl in the syn_{90} state relative to these three aromatic residues, as measured by its distance to their ring edges, is essentially the same as that of the α-keto carbonyl in FK506 (Table III). The indole ring of Trp 59 forms the bottom of the binding pocket; the substrate proline ring interacts favorably with Trp 59 with distances corresponding to those of the pipecolinyl ring of FK506 (see Table III).

Along the entire reaction path, the interaction energy between each individual FKBP residue and the whole substrate is stabilizing (except for residues that are too distant to interact). This indicates that the model is favorably positioned in the site. Most of the binding energy comes from residues engaged in hydrogen-bonding interactions with the substrate; the primary contributions come from Tyr 82, Asp 37, Glu 54, Val 55, and Ile 56 (see Figure 3).

Reaction Path and Activation Barrier. The type VIa turn model leads to a $cis_\zeta \rightarrow trans_\zeta$ reaction path of the "least action" type, in which there is very little structural change in the enzyme and the substrate. The angles ψ^{Leu} and ζ are the only substrate backbone torsion angles that change significantly (see Table I). As ζ increases, ψ^{Leu} decreases and the imide C=O group rotates around an axis through atoms C_α^{Leu} and N^{Pro} (see Figures 1C and 2), without any other major change in the substrate. At all points along the reaction path, the N- and C-terminal methyl groups of the substrate remain solvent accessible. Thus, a protein loop could bind and react with the same conformations as those involved in the tetrapeptide reaction path.

The potential energy along the adiabatic path of the $cis_\zeta \rightarrow trans_\zeta$ prolyl isomerization is shown in Figure 4. The total energy, the self-energy of the substrate, that of FKBP, and the substrate/FKBP interaction energy are shown. The barrier maximum, ΔE^*, at $\zeta = 43°$ is equal to 5.7 kcal/mol, relative to the cis_ζ reactant; slightly different models yield a variation in the barrier of ±1 kcal/mol and a variation in the angle ζ of ±3°.[5] The enzyme/substrate complex is not stable in the planar *cis* form ($\zeta = 0$). The decrease in binding energy along the reaction path leads to the cis_ζ minimum at $\zeta = 25°$; the substrate is destabilized by 2.3 ± 0.5 kcal/mol, and the binding energy changes by −2.8 ± 1.1 kcal/mol. Further distortion of the imide bond, in going to syn_{90}, increases the substrate energy by 9.9 ± 0.3 kcal/mol, which is partially balanced by a further drop in the binding energy of −3.7 ± 1.7 kcal/mol. The overall decrease in binding energy between the planar *cis* form and syn_{90} is −6.5 ± 0.5 kcal/mol and the overall substrate destabilization is 12.1 ± 0.2 kcal/mol. The contribution of the changes in the self-energy of FKBP is small (−0.75 ± 0.3 kcal/mol). The decrease of the interaction energy at $\lambda \cong 0.33$ leads to an early transition state ($\zeta^* = 43 \pm 3°$), even though the substrate energy has its maximum close to $\zeta = 90°$ (see Figure 4).

The increase in energy due to substrate distortion (12.1 kcal/mol) at syn_{90} is significantly smaller than the intrinsic *cis* → *trans* barrier of 15.7 kcal/mol obtained with the same potential energy function for the isolated proline dipeptide. The difference is accounted for by ground-state destabilization and substrate autocatalysis. The *ab initio* calculations show that the height of the *cis* to *trans* imide torsion barrier varies by 5.8 kcal/mol as a function of ψ^{Pro} from a minimum at ψ^{Pro} near 0° to a maximum at ψ^{Pro} near 150°. When the imide bond is twisted into the transition state, the imide nitrogen becomes pyramidal and its sp^3 lone pair forms a net dipole oriented perpendicular to the plane of the three ligands bound to the nitrogen (Wiberg & Laidig, 1987). With $\psi^{Pro} \approx 0°$, the amide hydrogen of the Phe forms a hydrogen bond with the lone pair of the imide nitrogen (Figure 1c), whereas when $\psi^{Pro} \approx 180°$, the proximal amide oxygen points toward the lone pair, resulting in an unfavorable interaction. The term "autocatalysis" is used for the stabilization of the substrate by the formation of the imide lone-pair hydrogen bond in the transition state. The imide torsion barrier of *N*-acetylpyrrolidine lacks the stabilizing NH group of proline dipeptide and therefore does not have an autocatalysis contribution; its *ab initio* barrier at the 6-31G* level is 1.4 kcal/mol higher than that of proline dipeptide computed with the same basis set. For an isolated proline dipeptide, the stable *cis* conformer and the *syn* transition state both have ψ^{Pro} near 0°. The distorted cis_ζ tetrapeptide bound to FKBP has $\psi^{Pro} = 38°$, which significantly raises the energy. As the reaction proceeds, ψ^{Pro} gradually decreases and reaches 14° at syn_{90} (see Table I). Thus, the energy of the proline dipeptide moiety of the substrate is raised more in the reactant state (cis_ζ) than in the syn_{90} state, and the effective activation barrier is decreased by approximately 3.6 kcal/mol.

For the *trans* → *cis* reaction, the situation is more complex due to the presence of two bound *trans* substrate minima, $trans_{180}$ and $trans_\zeta$. In $trans_{180}$, the proline dipeptide moiety adopts a (ζ,ψ^{Pro}) conformation similar to that of the isolated *trans* proline dipeptide, which has $(\zeta,\psi^{Pro}) = (186°, 68°)$ and forms the same type of seven-membered hydrogen-bonded ring as $trans_{180}$. In $trans_\zeta$, the H-bond is broken and ζ is twisted from 200° to 137°, with a substrate energy increase of 7.3 ± 1.2 kcal/mol. This destabilization is compensated

[5] The limits on energies and geometric variables given in the text and the tables correspond to the variations observed in models with somewhat differing substrate side-chain orientations; they do not correspond to standard errors.

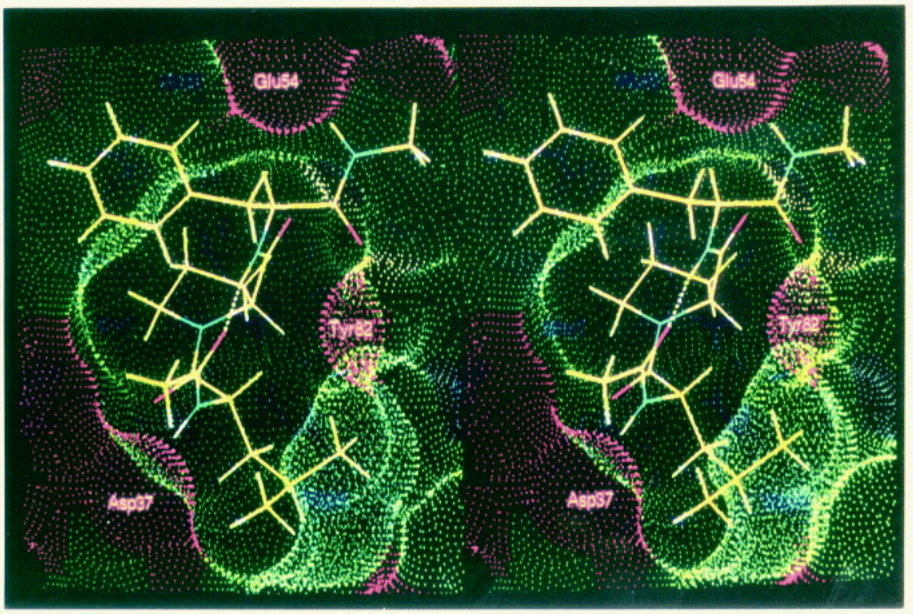
Glu54
Tyr82
Asp37
Glu54
Tyr82
Asp37

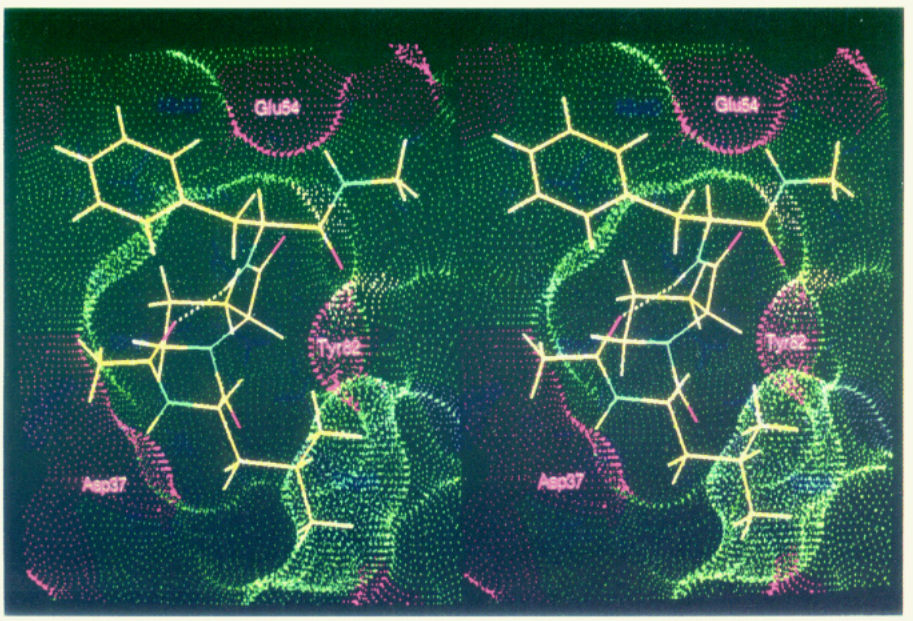
Glu54
Tyr82
Asp37
Glu54
Tyr82
Asp37

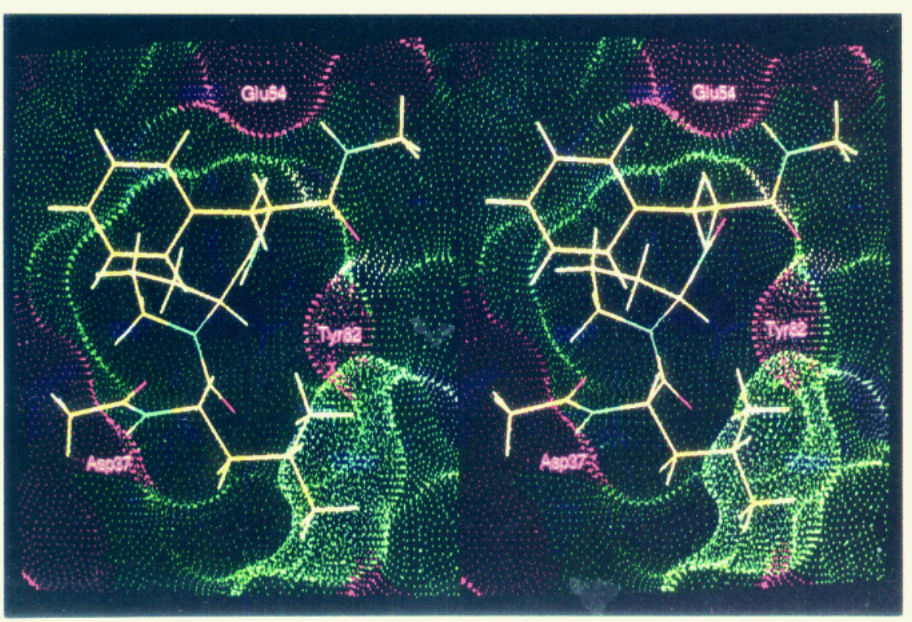
Glu54
Tyr82
Asp37
Glu54
Tyr82
Asp37

FIGURE 2: Stereoview of the Leu-Pro-Phe tetrapeptide bound to FKBP in the type VIa turn conformation: (A, top) reactant, cis_ζ; (B, middle) an intermediate point, syn_{90}; (C, bottom) product, $trans_\zeta$; see text. Stick representation of the substrate and Connolly surface (probe 1.5 Å) of the FK506 binding pocket of FKBP. Enzyme carbons are in green, substrate carbons in yellow, oxygens in red, nitrogens in blue, and polar hydrogens in white.

Table II: Hydrogen Bond Distances (Å) from FKBP to the Substrate or to FK506[a]

H-bond partners					
FKBP	tetrapeptide	cis_ζ	syn_{90}	$trans_\zeta$	FK506
Glu 54 amide O	C-terminus amide H	1.82 (0.03)	1.81 (0.03)	1.85 (0.04)	2.18
Ile 56 amide H	Pro amide O	2.22 (0.04)	2.10 (0.02)	2.15 (0.06)	1.92
Tyr 82 hydroxyl H	Phe amide O	1.63 (0.01)	1.63 (0.01)	1.61 (0.01)	1.87
Asp 37 carboxylate O	Leu amide H	1.81 (0.05)	1.72 (0.01)	1.72 (0.01)	1.74
	intrasubstrate Phe amide H to N-terminus amide O	1.90 (0.02)	1.96 (0.03)	3.72 (0.6)	

[a] The FK506 values are based on the crystal structure. See also footnote of Table I.

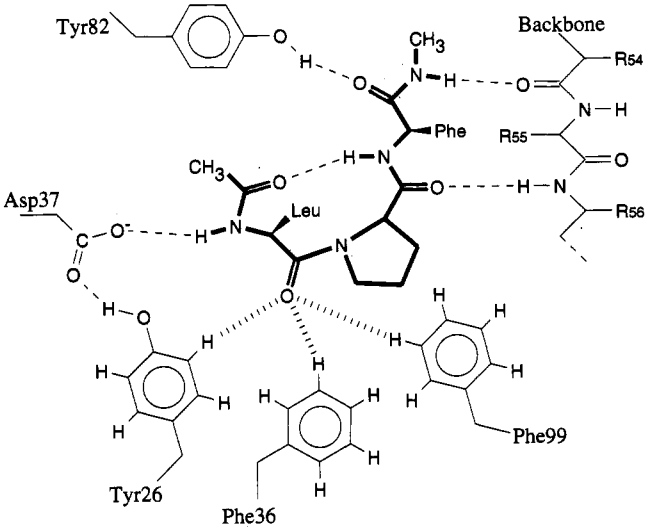

FIGURE 3: Schematic representation of the H-binding pattern and the carbonyl/aromatic interactions of the type VIa turn model. Side-chains: R54 = Glu, R55 = Val, and R56 = Ile.

Table III: Important Distances (Å) from FKBP to the Substrate or to FK506[a]

	tetrapeptide			
FKBP	cis_ζ	syn_{90}	$trans_\zeta$	FK506
$C_{\epsilon 2}^{Trp59\ b}$	3.21 (0.07)	3.02 (0.01)	3.22 (0.3)	2.74
$H_{\delta 1}^{Tyr26\ c}$	2.80 (0.02)	3.99 (0.2)	4.69 (0.2)	2.73
$H_{\beta 2}^{Phe36\ c}$	4.00 (0.3)	2.57 (0.02)	2.70 (0.01)	2.43
$H_{\epsilon 2}^{Phe99c}$	3.16 (0.3)	2.56 (0.1)	3.14 (0.03)	2.53

[a] The FK506 values are based on the crystal structure. See also footnote of Table I. [b] From the Trp59 indole ring ($C_{\epsilon 2}$) to the edge of either the tetrapeptide proline ring ($H_{\beta 1}$) or the FK506 pipecolinyl ring ($H_{\beta 1}$). [c] From the edge of the aromatic ring to either the tetrapeptide imide carbonyl oxygen (O^{Leu}) or the FK506 C9 keto-carbonyl oxygen.

by a large decrease in the binding energy (–6.2 ± 1 kcal/mol), so that the two *trans* conforms have nearly the same total energy. The activation barrier for the $trans_{180} \rightarrow trans_\zeta$ conversion is 5.6 ± 1.1 kcal/mol, similar in magnitude to the barrier for the $trans_\zeta \rightarrow cis_\zeta$ isomerization (5.3 ± 0.9 kcal/mol). Just as for the $cis_\zeta \rightarrow syn_{90}$ barrier, the substrate component of the $trans_{180} \rightarrow syn_{90}$ barrier (12.1 ± 2.4 kcal/mol) is much smaller than the barrier in the isolated proline dipeptide. Most of the difference is due to the concurrent formation of the intrasubstrate hydrogen bond which closes the 10-membered ring as the system goes from the $trans_\zeta$ to the syn_{90} state (see Table II); this hydrogen bond contributes a stabilization of –3.9 ± 0.1 kcal/mol. If substrate dissociation and rebinding are fast, the $trans_{180} \rightarrow trans_\zeta$ conversion could

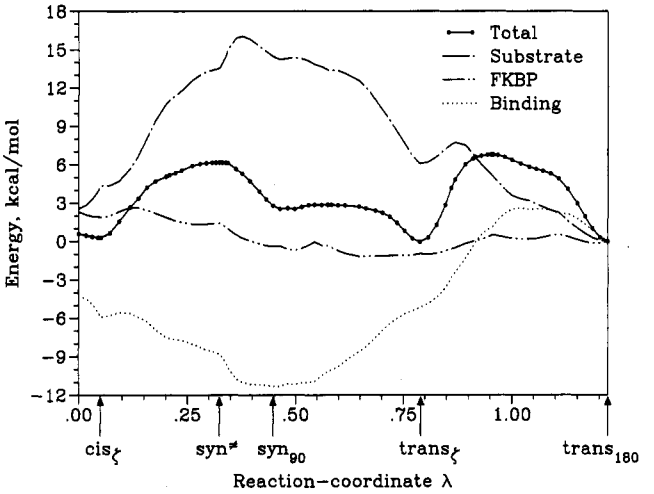

FIGURE 4: Adiabatic energy profile of the *cis* → *trans* proline isomerization path, obtained with the structures displayed in Figure 2. The total potential energy (·—·) is broken down into its three components: the self-energy of the substrate (– · –), the self-energy of the enzyme (– ·· –), and the FKBP/substrate interaction energy (···). The cis_ζ, syn^*, syn_{90}, and $trans_{180}$ conformers are located with arrows (see Table I for values of ζ at these points). The path connecting them was obtained by CPR/SCM refinement (as described in the Methods section), and the path segment from cis_ζ to $\lambda = 0$ was computed by adiabatic distortion of ζ, for a total of 77 intermediate structures (•). λ is the real one-dimensional reaction coordinate, measuring the progress along the path by summing the $\partial\lambda = |\mathbf{q}_{i+1} - \mathbf{q}_i|$, which is the RMS of the coordinate difference between two successive intermediates along the path. It is normalized here, so that $\lambda = 0$ and $\lambda = 1$ are the intermediates which have $\zeta = 0$ (substrate completely *cis*) and $\zeta = 180$ (fully *trans*), respectively. Expressed in RMS of coordinate differences, the distance along the path from $\lambda = 0$ to $\lambda = 1$ is 0.92 Å, whereas the direct distance is 0.29 Å. Energies are relative to the $trans_{180}$ state.

proceed via a dissociation mechanism since there is no barrier in solution; $trans_{180}$ would then be an unproductive binding mode.

The important residues contributing to substrate stabilization in the transition state, relative to the reactant state, depend on whether the reactant is a *cis* or *trans* proline (see Figure 2). For the isomerization starting with the *cis* conformer, the dominant contributions come from the interaction of Asp 37 and Phe 36 with the imide C=O group; smaller contributions come from Tyr 26 and Phe 46. For the reaction starting with the *trans* conformer, more side chains are involved. Tyr 82 and Ile 56 are most important, with smaller contributions from Phe 99, Tyr 26, Phe 36, Glu 54, and Trp 59. Again, the interactions with the imide carbonyl make the dominant contribution.

The residues implicated in catalysis are in agreement with the observed effects of FKBP point mutations on the *cis* →

trans isomerization. Specifically, mutations of several residues distal to the FK506 binding pocket do not affect rotamase activity (Park *et al.*, 1992), nor did H87A (Yang *et al.*, 1993) and H87V (Aldape *et al.*, 1992). All of these are not involved in the proposed mechanism. The mutant D37V is inactive, in accord with the essential role of Asp 37. Mutation of Tyr 82 to Phe would be expected to significantly alter the *trans* → *cis* catalysis.

DISCUSSION

The main result of the present study is the proposal that the substrate binds as a type VIa proline turn and that rotamase catalysis by FKBP is achieved by a combination of factors, each of which makes a significant contribution to the lowering of the prolyl isomerization barrier. They are a decrease of the intrinsic barrier by desolvation of the reacting imide group and substrate autocatalysis, destabilization of the reactant, and preferential transition-state binding.

Imide Desolvation and Substrate Autocatalysis. The 15.7 kcal/mol barrier for the isomerization of an isolated proline dipeptide in vacuum is about 3.3 kcal/mol lower than the experimental enthalpy of activation for water-solvated peptidylprolines (Albers *et al.*, 1990). This is in accord with experimental studies (Calzolari *et al.*, 1970; Drakenberg *et al.*, 1972; Eberhardt *et al.*, 1992) and with quantum mechanical calculations that have shown that hydrogen bonds between water and *N*-methylacetamide increase the C—N π-bond overlap population (Scheiner & Kern, 1977; Guo & Karplus, 1992). The effect of one to four water molecules interacting with the carbonyl oxygen leads to an increase of 2–5 kcal/mol in the *cis* → *trans* amide torsion barrier (Scheiner & Kern, 1977).

In the enzyme/substrate complex the imide carbonyl is the only acceptor of the substrate which does not form a hydrogen bond along the adiabatic reaction path. This has the two-fold effect that no hydrogen bond is lost in going from the reactant to the transition state and that the intrinsic isomerization barrier is not raised by solvent polarization of the imide carbonyl. In the transition state the imide carbonyl points toward the core of an apolar binding pocket, which is formed by the aromatic side chains of Tyr 26, Phe 36, and Phe 99. There are stabilizing polar C—H···O interactions (see below). However, these are much weaker than hydrogen bonds with water, so that a barrier lowering to near the vacuum value is expected.

An additional contribution to the low intrinsic barrier comes from substrate autocatalysis. As the imide bond is twisted, the system is stabilized because the NH of Phe forms a hydrogen bond with the lone pair of the pyramidilized imide nitrogen in the type VIa turn stabilized by the enzyme. The importance of this contribution to the rotamase mechanism might be investigated experimentally by measuring the effect on the activation enthalpy of a modification of the substrate from a prolylphenyl amide, -Pro-NH-Phe-, to a prolylphenyl ester, -Pro-O-Phe-, which lacks the hydrogen needed to interact with the imide lone pair. An increase in the activation enthalpy for the ester substrate relative to the amide substrate would be in agreement with the present model. Similarly, imide isomerization of the first proline in a -Pro-Pro-containing substrate, which also lacks the relevant hydrogen, would be expected to be less well catalyzed by FKBP. However, both of these modifications of the substrate might have other effects as well (e.g., a change in the binding geometry or in the activation entropy).

Ground-State Destabilization. As shown in Figure 4, FKBP favors the binding of the twisted *syn* intermediate over both the *cis* and *trans* forms of the substrate. Part of this decrease in binding energy is used to destabilize the two ground states, either by directly twisting the imide bond (ζ goes from 0° to 25° on the *cis* side and ζ goes from 180° to 137° on the *trans* side) or by increasing the substrate energy in other ways (the angle ψ^{Pro} is shifted from 0° to 38° in *cis* and the 10-membered intrasubstrate ring is broken by distortion in *trans*). Distortion of the imide bond has been reported for a *cis* peptidylprolyl substrate bound to cyclophilin (Kallen & Walkinshaw, 1992). Two residues, Asp 37 and Tyr 82, contribute most of the decrease in binding energy at syn_{90}, relative to *cis* and *trans*, respectively. The dominant effect arises from the repulsive interactions of these two residues with the imide carbonyl in the initial *cis* or *trans* states. This results in ground-state destabilization (imide twist in cis_ζ and $trans_\zeta$), as indicated pictorially in Figure 2A,C. The carboxylate oxygen of Asp 37 and the hydroxyl oxygen of Tyr 82 are across from each other in the binding pocket on the two sides of the (C_α^{Leu} – N^{Pro}) carbonyl rotation axis. Both repel the imide carbonyl oxygen (Asp 37 by 1.6 kcal/mol in planar *cis* and Tyr 82 by 2.1 kcal/mol in planar *trans*) and act to distort the imide bond toward syn_{90}, in which the carbonyl oxygen points away from both Asp 37 and Tyr 82.

Preferential Transition-State Binding. The interaction between the substrate and FKBP also stabilizes the transition state in accord with the classic ideas of Pauling (1946) and Fersht (1985). As suggested by Van Duyne *et al.* (1991, 1993) C—H···O interactions between the side chains of the aromatic triad and the imide carbonyl contribute to transition-state stabilization. The planar *cis* → syn_{90} change in interaction energy between these residues and the imide carbonyl is –1.5 kcal/mol; for planar *trans* → syn_{90}, the change is –2.3 kcal/mol. Thus, transition-state binding makes a relatively small contribution in this case.

Catalysis Mechanism of Cyclophilin. The structure proposed here for the substrate bound to FKBP differs significantly from the X-ray structure found for the -Ala-Pro-Ala- peptide bound to cyclophilin (Kallen & Walkinshaw, 1992). The latter adopts the conformation of a type VIb turn, which differs from the type VIa turn proposed for FKBP in that $\psi^{Pro} \approx 150°$ instead of being near 0°. Consequently, the amide hydrogen of the Ala residue that corresponds to the Phe of the FKBP substrate cannot interact with the sp^3 lone pair of the twisted imide nitrogen, and a high internal barrier would be expected. However, in cyclophilin, in contrast to FKBP, there is an arginine in the binding pocket that could interact with the nitrogen lone pair, in analogy to the *cis* → *trans* isomerization catalysis observed in dihydrofolate reductase (Texter *et al.*, 1992). Thus, although substrate distortion is observed in cyclophilin (Kallen & Walkinshaw, 1992), the present model for the catalytic mechanism of FKBP suggests that cyclophilin catalysis may differ in some details from that in FKBP.

Binding Motifs. Cis prolines are found primarily in bends and turns (Stewart *et al.*, 1990), which are often exposed at the surface of proteins and adopt either the type VI a or b conformation (Müller *et al.*, 1993). If it is assumed that rotamases are needed to accelerate the folding of proteins that are in a compact globule state in which the local secondary structure of proline turns is already defined, it is plausible that two distinct classes of rotamases would evolve, such as the FKBPs and the cyclophilins, each adapted to catalyzing the isomerization of one of these two types of proline turns. It is also worth noting that the substrate specificity of FKBP for bulky non-β-branched residues preceding the proline is in accord with the statistical preference for tyrosines and leucines in that position among naturally occurring *cis* prolines

(Richardson & Richardson, 1989; McArthur & Thornton, 1991). In addition to their role as rotamases, immunophilins have been postulated to prevent aggregation of partially unfolded proteins (Gething & Sambrook, 1992), to act as scaffolding in macromolecular assemblies (Jayaraman *et al.*, 1992; Tai *et al.*, 1993), and to stabilize proteins during processing and secretion from cells (Stamnes & Zuker, 1990). Recognition of specific type VI prolylpeptide turns on the surface of proteins may be important here as well.

NOTE ADDED IN PROOF

Support for the model for the bound *trans* and transition state proposed in Fischer (1992) and used in this paper is provided by the crystal structure of a cyclic FK506/peptide hybrid bound to FKBP recently determined by Y. Ikeda, L. W. Schultz, J. Clardy, and S. L. Schreiber (personal communication, November 1993). The hybrid molecule contains the essential FK506 pipecolinyl and dicarbonyl moieties (atoms 2–9 in Figure 1A), on each side of which the chain extends as an α-amino polypeptide. Four essential features of the model are confirmed by the cocrystal structure: (1) The pipecolinyl-peptide ψ (corresponding to ψ^{Pro} in our model) is about 10°, which brings the down-chain amide within hydrogen-bonding distance of the imide nitrogen (N7) and allows the formation of a hydrogen bond to the "i – 2" up-chain carbonyl, resulting in a type VIa turn structure. (2) The stretch of antiparallel β-sheet between the macrocycle and residues 54–56 of FKBP is present. (3) The hydroxyl group of Tyr 82 hydrogen bonds to the second amide down-chain of the macrocycle instead of to the pipecolinyl imide carbonyl as in the FK506/FKBP cocrystal structure. (4) The *trans* imide C8 carbonyl is not involved in any hydrogen bond, an essential feature of the proposed rotamase mechanism.

ACKNOWLEDGMENT

We thank Michael Sommer for his assistance with the pK_a estimations, Amedeo Caflisch for doing the Poisson–Boltzmann calculations, and Roland Dunbrack for doing most of the *ab initio* calculations. We also thank Stuart L. Schreiber for helpful discussions. The calculations were performed on a Convex C220 and a Silicon Graphics 4D/340.

REFERENCES

Albers, M. W., Walsh, C. T., & Schreiber, S. L. (1990) *J. Org. Chem. 55*, 4984.

Aldape, R. A., Futer, O., DeCenzo, M. T., Jarrett, B. P., Murcko, M. A., & Livingston, D. J. (1992) *J. Biol. Chem. 267*, 16029.

Bash, B. A., Field, M. J., Davenport, R. C., Petsko, G. A., Ringe, D., & Karplus, M. (1991) *Biochemistry 30*, 5826.

Bashford, D., & Karplus, M. (1990) *Biochemistry 29*, 10219.

Brandts, J. F., Halvorson, H. R., & Brennan, M. (1975) *Biochemistry 14*, 4953.

Brooks, B. R., Bruccoleri, R. E., Olafson, B. D., States, D. J., Swaminathan, S., & Karplus, M. (1983) *J. Comput. Chem. 4*, 187.

Brooks, C. L., III, Karplus, M., & Pettitt, B. M. (1988) Proteins: a theoretical perspective of dynamics, structure and thermodynamics, in *Advances in Chemical Physics*, Vol. 71, John Wiley & Sons, New York.

Calzolari, A., Cont, F., & Franconi, C. (1970) *J. Chem. Soc. B 55*, 555.

Choi, C., & Elber, R. (1991) *J. Chem. Phys. 94*, 751.

Davis, M. E., & McCammon, J. A. (1990) *J. Comput. Chem. 11*, 401.

Desiraju, G. R. (1991) *Acc. Chem. Res. 24*, 290.

Drakenberg, T., Dalquist, K.-I., & Forsén, S. (1972) *J. Phys. Chem. 76*, 2178.

Eberhardt, E. S., Loh, S. N., Hinck, A. P., & Raines, R. T. (1992) *J. Am. Chem. Soc. 114*, 5437.

Fersht, A. (1985) *Enzyme Structure and Mechanism*, 2nd ed., W. H. Freeman & Co., New York.

Fischer, S. (1992) Curvilinear reaction coordinates of conformational change in macromolecules. Application to rotamase catalysis, Ph.D. Thesis, Harvard University, Cambridge, MA.

Fischer, G., & Schmid, F. X. (1990) *Biochemistry 29*, 2205.

Fischer, S., & Karplus, M. (1992) *Chem. Phys. Lett. 194*, 252.

Fischer, G., Wittmann-Liebold, B., Lang, K., Kiefaber, T., & Schmid, F. X. (1989) *Nature 337*, 476.

Freedman, R. B. (1992) in *Protein Folding* (Creighton, T. E., Ed.) W. H. Freeman & Co., New York.

Frisch, M. J., Trucks, G. W., Head-Gordon, M., Gill, P. M. W., Wong, M. W., Foresman, J. B., Johnson, B. G., Schlegel, H. B., Robb, M. A., Replogle, E. S., Gomperts, R., Andres, J. L., Raghavachari, K., Binkley, J. S., Gonzalez, C., Martin, R. L., Fox, D. J., Defrees, D. J., Baker, J., Stewart, J. J. P., & Pople, J. A. (1992) *Gaussian 92 Revision C*, Gaussian, Inc., Pittsburgh, PA.

Gething, M.-J., & Sambrook, J. (1992) *Nature 355*, 33.

Gilson, M. K., & Honig, B. H. (1988) *Proteins 3*, 32.

Guo, H., & Karplus, M. (1992) *J. Phys. Chem. 96*, 7273.

Harrison, R. K., & Stein, R. L. (1990a) *Biochemistry 29*, 1684.

Harrison, R. K., & Stein, R. L. (1990b) *Biochemistry 29*, 3813.

Harrison, R. K., & Stein, R. L. (1992) *J. Am. Chem. Soc. 114*, 3464.

Jayaraman, T., Briliantes, A.-M., Timmerman, A. P., Fleischer, S., Erdjument-Bromage, H., Tempst, P., & Marks, A. R. (1992) *J. Biol. Chem. 267*, 9474.

Kallen, J., & Walkinshaw, M. D. (1992) *FEBS Lett. 300*, 286.

Kofron, J. L., Kuzmic, P., Kishore, V., Colon-Bonilla, E., & Rich, D. H. (1991) *Biochemistry 30*, 6127.

MacArthur, M. W., & Thornton, J. M. (1991) *J. Mol. Biol. 218*, 397.

Müller, G., Gurrath, M., Kurz, M., & Kessler, H. (1993) *Proteins 15*, 235.

Park, S. T., Aldape, R. A., Futer, O., DeCenzo, M. T., & Livingston, D. J. (1992) *J. Biol. Chem. 267*, 3316.

Pauling, L. (1946) *Chem. Eng. News 24*, 1792.

Richardson, J. S., & Richardson, D. C. (1989) in *Prediction of protein structure and the principles of protein conformation* (Fasman, G. D., Ed.) Plenum, New York.

Rosen, M. K., Standaert, R. F., Galat, A., Nakatsuka, M., & Schreiber, S. L. (1990) *Science 248*, 863.

Schneider, S., & Kern, C. W. (1977) *J. Am. Chem. Soc. 99*, 21.

Schreiber, S. L. (1991) *Science 251*, 283.

Schreiber, S. L., & Crabtree, G. R. (1992) *Immunol. Today 13*, 136.

Stamnes, M. A., & Zuker, C. S. (1990) *Curr. Opin. Cell Biol. 2*, 1104.

Stein, R. L. (1993) *Adv. Protein Chem. 44*, 1.

Stewart, D. E., Sarkar, A., & Wampler, J. E. (1990) *J. Mol. Biol. 214*, 253.

Tai, P.-K., Chang, H., Albers, M. W., Schreiber, S. L., Toft, D. O., & Faber, L. E. (1993) *Biochemistry 32*, 8842.

Texter, F. L., Spencer, D. B., Rosenstein, R., & Mathews, C. R. (1992) *Biochemistry 31*, 5687.

Trandinh, C. C., Pao, G. M., & Saier, M. H., Jr. (1992) *FASEB J. 6*, 3410.

Tropschug, M., Wachter, E., Mayer, S., Schonbrunner, E. R., & Schmid, F. X. (1990) *Nature 346*, 674.

Van Duyne, G. D., Standaert, R. F., Karplus, P. A., Schreiber, S. L., & Clardy, J. (1991) *J. Mol. Biol. 229*, 105.

Van Duyne, G. D., Standaert, R. F., Karplus, P. A., Schreiber, S. L., & Clardy, J. (1993) *Science 252*, 839.

Wiberg, K. B., & Laidig, K. E. (1987) *J. Am. Chem. Soc. 109*, 5935.

Wolfenden, R., & Radzicka, A. (1991) *Chemtracts: Biochem. Mol. Biol. 2*, 52.

Yang, D., Rosen, M. K., & Schreiber, S. L. (1993) *J. Am. Chem. Soc. 115*, 819.